THE JOURNAL OF PHYSICAL CHEMISTRY LETTERS
A JOURNAL OF THE AMERICAN CHEMICAL SOCIETY

pubs.acs.org/JPCL

Letter

# Energetics, Interlayer Molecular Structures, and Hydration Mechanisms of Dimethyl Sulfoxide (DMSO)−Kaolinite Nanoclay Guest−Host Interactions

Jie Wang, Liangjie Fu,* Huaming Yang,* Xiaochao Zuo, and Di Wu

Cite This: *J. Phys. Chem. Lett.* 2021, 12, 9973−9981

Read Online

ACCESS | Metrics & More | Article Recommendations | Supporting Information

**ABSTRACT:** Two-dimensional (2D) kaolinite nanoclay is an important natural mineral with promising application potential, especially tuned with organic intercalates. However, thus far, the organics−kaolinite guest−host interactions, the atomic scale structures of organic intercalates under confinement, and molecular level mechanisms of hydration are rarely systematically explored using both experimental and computational methodologies. We integrated density functional theory with dispersion scheme (DFT-D) with various experimental methods to investigate the intercalation of dimethyl sulfoxide (DMSO) in kaolinite with and without hydration. The kinetic, thermodynamic, and structural impacts of hydration were highlighted. In short, water molecules significantly promote intercalation of DMSO into kaolinite because of favorable intercalation energy, which is enabled by effective hydrogen bonding at the guest species (DMSO and water)−kaolinite interfaces.

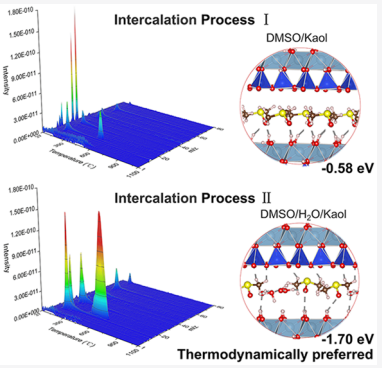




Intercalation and exfoliation are effective strategies to synthesize nanoscale materials with tunable structures and functionality.[1−5] For 2D materials, intercalation leads to significant modifications in structural, morphological, interfacial, and rheological properties.[6−11] Kaolinite is one of the critical 2D nanoclay minerals which has been extensively applied in polymer,[12] heterogeneous catalysis,[13,14] energy storage,[15,16] organic pollutants and heavy metals separation,[17] and biomedicine.[18,19] Other than interlayer van der Waals interactions, the kaolinite layers are assembled and stacked together by hydrogen bonding (Figure 1). As a result, only a limited number of organic molecules featuring strong hydrogen bonding with kaolinite can be intercalated into its interlayer space, including hydrazine, formamide, potassium acetate, urea, dimethyl-sulfoxide (DMSO), and *N*-methylformamide.[20] DMSO is the most common guest species for kaolinite intercalation, and the DMSO−kaolinite interlayer complexes could be employed as precursors for further modification of kaolinite with organic compounds.[21,22] Hence, fundamental understanding on the energetics of DMSO−kaolinite interfacial interactions, and atomic scale structures of the complexes is important for the applications of kaolinite.

Typically, the cost of the intercalation and exfoliation of kaolinite is high, mainly because the rates of organics intercalation and the subsequent delamination between kaolinite layers are low. Existing experimental studies focusing on material synthesis and kinetics suggest that hydration enhances the intercalation rates of organics. Olejnik et al. found that the intercalation pathways of DMSO in kaolinite could be substantially facilitated under the presence of water.[23] Makó et al. introduced a small amount of distilled water to age kaolinite prior to DMSO intercalation.[24] Interestingly, the yield intercalation was boosted from 57% for anhydrous kaolinite to 89% for hydrated kaolinite. Abou-El-Sherbini et al. demonstrated that hydration enhanced DMSO intercalation rates and led to unexpected kaolinite exfoliation.[24] Moreover, it was also observed in different studies that hydration promoted the intercalation of other small molecules, including potassium acetate,[25] methanol,[26] hydrazine,[25] *N*-methylformamide,[27−30] and urea.[24] However, systematic mechanistic studies on the effects of hydration (interlayer water) on DMSO intercalation kinetics and thermodynamics (energetics and structures) have been rarely carried out.[31]

The DMSO−kaolinite interactions have been mostly studied using spectroscopic and structural methods.[32−35] Specifically, Frost et al. identified symmetric and antisymmetric modes of intercalated DMSO in kaolinite using FTIR and Raman spectra, including monomeric, polymeric, and nonbonded DMSO under interlayer confinement.[33] Abou-El-Sherbini et al.[34] proposed two mechanisms of DMSO intercalation in kaolinite, including (i) indirect hydrogen bonding of DMSO to exfoliated kaolinite silica layers via an intermediate water layer

**Received:** August 19, 2021
**Accepted:** September 15, 2021
**Published:** October 7, 2021

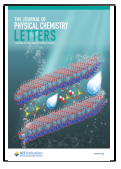

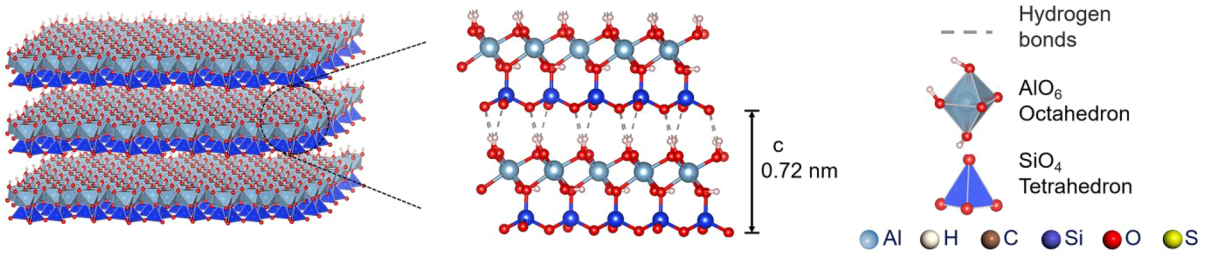


**Figure 1.** Schematic illustration of kaolinite.

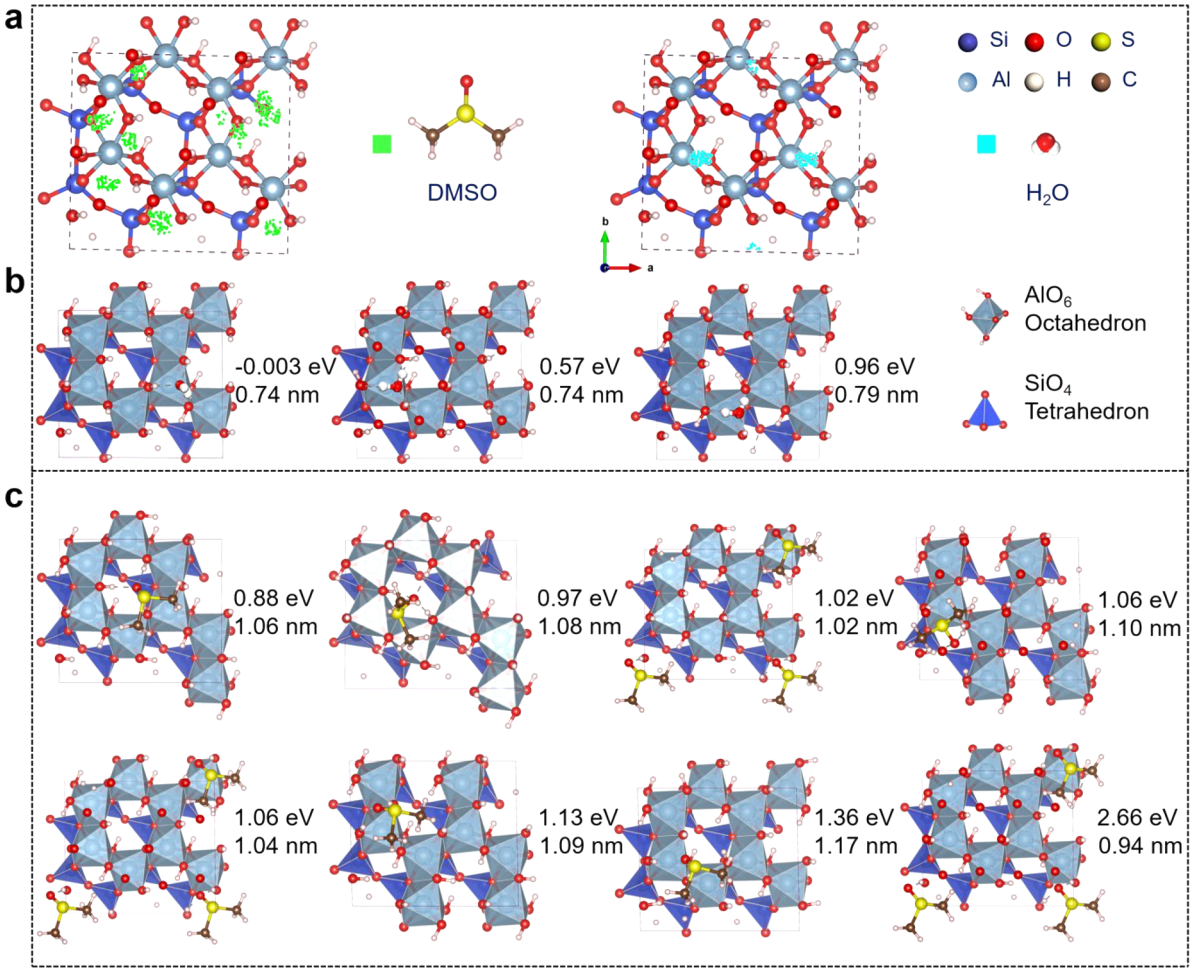


**Figure 2.** (a) Active intercalation sites of DMSO and water molecules in kaolinite. The optimized configurations with (b) one water and (c) one DMSO. The preferential intercalation sites are highlighted in neon green and cyan in panel a. The magnitudes of intercalation energy and basal spacings are given for all configurations in panels b and c.

and (ii) direct hydrogen bonding, in which DMSO binds to kaolinite inner−surface aluminol groups. Yariv et al.[35] studied DMSO−kaolinite complexes by thermo−IR−spectroscopy, and two types of complexes were identified. The type I complex was present up to 120 °C with intercalated water bridged between DMSO and the clay−O−planes; the type II complex was obtained by the thermal escape of the intercalated water between 130 and 150 °C.

Recently, the structural and thermodynamic evolutions of kaolinite during the intercalation process have been studied by computational methods at atomic scales. Using molecular dynamics (MD), Zhang et al. studied potential structures of intercalated molecules under kaolinite confinement.[21,36] Molecular assemblage of DMSO in the interlayer space of kaolinite is monolayer instead of bilayer.[36] It was also proposed that both the octahedral and tetrahedral surfaces of kaolinite featured affinity to DMSO to enable intercalation, and compared with the tetrahedral surface, the octahedral surface had stronger affinity with more exothermic interaction energies.[21] However, although the MD calculations using classical force field could mimic the guest−host interactions between kaolinite layers and DMSO molecules, the accurate description of their bonding structures and thermodynamics within the interlayer space is still a challenge. Furthermore, quantum chemical and DFT calculations were used to direct intercalation mechanism and structures of kaolinite with DMSO. Quantum chemical calculation was used to indicate the formations and orientations of hydrogen bonds between



https://doi.org/10.1021/acs.jpclett.1c02729
J. Phys. Chem. Lett. 2021, 12, 9973−9981

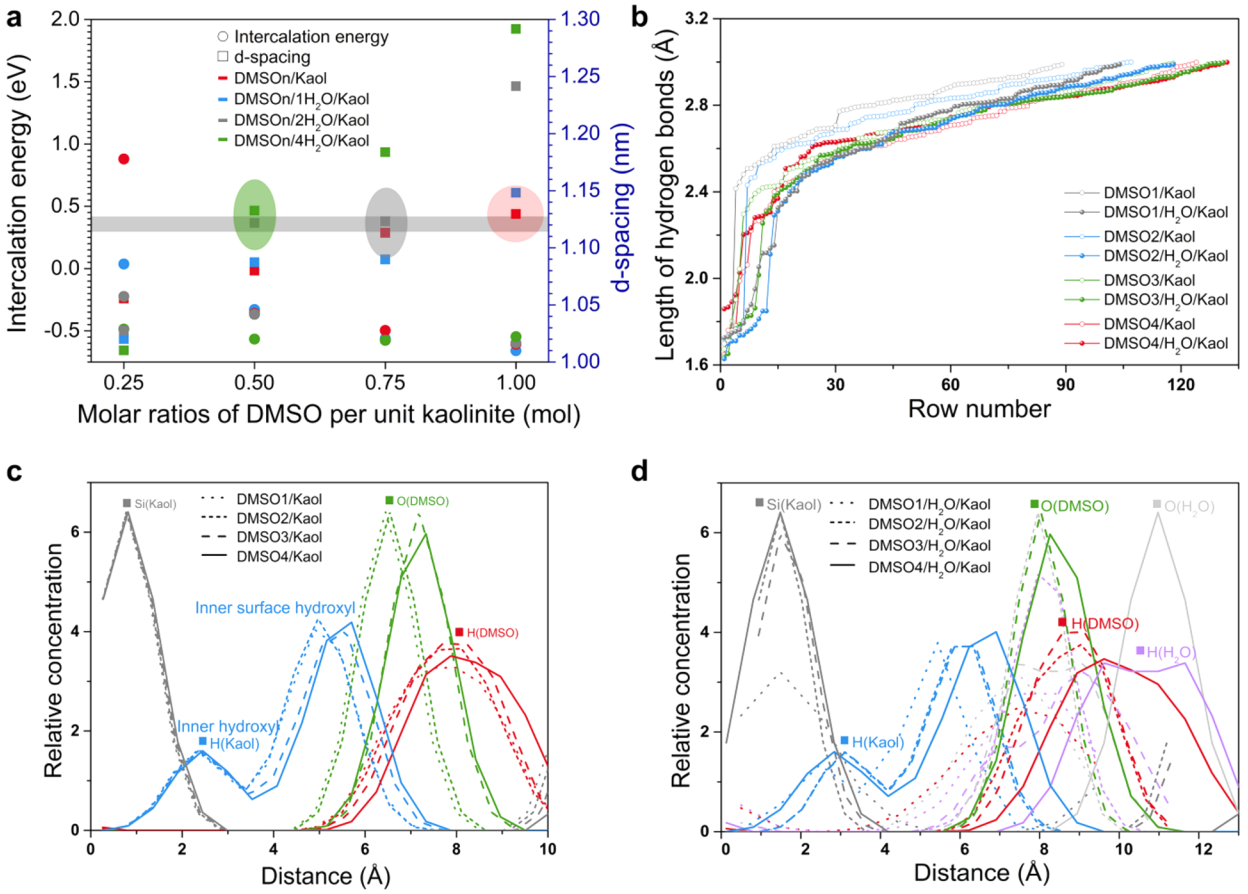


**Figure 3.** (a) Intercalation energy and interplanar *d*-spacing of DMSOn/Kaol and DMSOn/m$H_2O$/Kaol (energy is for per molecule, IE = $\Delta E/(m + n)$). The gray area corresponds to the *d*-spacing around 1.12 nm according to experiment results. The most possible structures are highlighted in large circles. (b) Length of hydrogen bonds of DMSOn/Kaol and DMSOn/m$H_2O$/Kaol. The number of hydrogen bond is denoted as "row number". (c) Relative concentration of atoms for DMSOn/Kaol. (d) Relative concentration of atoms for DMSOn/m$H_2O$/Kaol.

DMSO molecules and kaolinite layers.[37] Michalková confirmed that stable intercalates were formed with the hydrogen bonds between the sulfonyl oxygen atom and surface hydroxyl groups by DFT calculation, and the weak hydrogen bonds played an important role in the final localization and stabilization of the DMSO molecule in the interlayer space.[38] Although various DMSO intercalation mechanisms have been proposed, the accurate energetics and corresponding structures (kaolinite/DMSO/water) of intercalate−kaolinite guest−host system have not been clarified at atomic level using integrated experimental and computational methodologies, especially when water is involved.

In this study, we couple density functional theory (DFT) with Grimme's pairwise dispersion schemes (-D) combined with a series of experimental methodologies to investigate the (i) intercalation of DMSO in kaolinite as a function of guest molecule loading and (ii) the effects of hydration in governing the energetic driving force, structural specifics, and guest−host interactions of the DMSO−kaolinite system.

First, a 2 × 1 × 1 supercell was inserted with one water molecule and one DMSO molecule (0.25 mol DMSO per unit kaolinite). The active intercalation sites of kaolinite and structures of DMSO and water molecules under confinement, based on Monte Carlo simulation, are presented in Figure 2a. More specifically, the intercalation sites of DMSO and water molecules on kaolinite are primarily near Al−OH. It was pointed out by various reports that the S═O bond of DMSO forms hydrogen bonds with the hydroxyls of kaolinite.[36,38−40] On the basis of the Monte Carlo simulations, 3 compound configurations for water intercalation, and 8 for DMSO intercalation were chosen for further structural optimization. All atoms of the intercalated structures are fully relaxed. The intercalation energies and *d*-spacing (Figure 2b and c) of each configuration were calculated with DFT-D scheme, which describes the lattice parameters and formation energy of kaolinite better than traditional DFT functional as reported in previous works.[41,42] Specifically, the minimum intercalation energy of one DMSO molecule is 0.88 eV leading to a basal spacing of 1.06 nm. The lowest intercalation energy or hydration energy for a water molecule is −0.003 eV, resulting in an interlayer spacing of 0.74 nm. In this case the intercalation energy of DMSO is much higher than that of $H_2O$. Such phenomenon inconsistent with the experimental results was not anticipated. Generally, in experiments, the DMSO intercalation for kaolinite is spontaneously with negative intercalation energy and the *d*-spacing of DMSO intercalated kaolinite is 1.12 nm. Meanwhile, spontaneous water intercalation into the interlayer space of kaolinite is not achievable and the *d*-spacing of hydrated kaolinite layers is 0.84 nm. According to the intercalation energies, neither water nor DMSO could be directly intercalated within the interlayer spacing of kaolinite. Such discrepancy is likely because of the insufficient hydrogen bonding between one $H_2O$/DMSO molecule and kaolinite (0.25 mol DMSO per unit kaolinite).


https://doi.org/10.1021/acs.jpclett.1c02729
J. Phys. Chem. Lett. 2021, 12, 9973−9981

It is assumed that the total energetic cost is balanced by the more dense hydrogen bonding network when more DMSO and $H_2O$ molecules are intercalated into kaolinite during the solvent thermodynamics process.

Generally, the intercalation space is determined by the size and loading amount of intercalated guest species.[36] As such, the intercalated structures with DMSO/kaolinite molar ratio of 0.25, 0.50, 0.75, 1.00 without water were denoted as DMSOn/Kaol, while the structures with different degree of hydration were denoted as DMSOn/m$H_2O$/Kaol. The configurations and interaction energies of DMSOn/Kaol and DMSOn/m$H_2O$/Kaol are shown in Figures S1 and S2, respectively. Several configurations are tested for each model, among which the most possible structures are selected and presented in Figure 3a, and the lattice parameters and unit cell volumes are listed in Table S1. Table S2 details the calculated geometric parameters of free and intercalated DMSO molecules, which are in good agreement with the existing experimental results reported. When only DMSO is intercalated, as the DMSO content increases, the number or degree of hydroxyl bonding and electron transfer between DMSO and kaolinite both increase (Figure S1). As a result, the intercalation energy of DMSO per unit kaolinite tends to decrease (Figures 3a and S5). The same trend was observed by Michalkova et al.[40] As the DMSO/kaolinite molar ratio increases to 0.75, the layer spacing becomes 1.11 nm, which is in good agreement with the experimentally measured value of 1.12 nm. At DMSO/kaolinite molar ratio of 1.00, the energetically most favorable intercalation structure is achieved with a layer spacing of 1.12 nm. According to simultaneous TG−DTG−DTA experiments, there is one mole of DMSO per mole of inner−surface hydroxyl groups in the DMSO/Kaol complexes.[43] However, previous experiments results suggest that the DMSO/kaolinite molar ratio is mostly in the range of 0.4−1.0 (see Table S3). Additionally, the introduction of water promotes the intercalation of DMSO. In other words, it is very likely that water molecules participate in the intercalation energetically through stabilization of both DMSO and the internal surface of kaolinite.

The configurations of DMSO−kaolinite interactions with the presence of water are presented in Figure S2. Specifically, at the same DMSO loading, the calculated DMSO intercalation energies are significantly lower than the cases without water and the stability of DMSO and $H_2O$ molecules in DMSOn/m$H_2O$/Kaol structures are strongly influenced by each other (see Figure 3a and Table 1). Under hydration, the total intercalation energy reaches a minimum of −3.40 eV at a molar ratio of 0.50 (DMSO2/4$H_2O$/Kaol) while intercalation energy per molecule of DMSO/$H_2O$ for DMSO loading amount higher than 0.50 are mostly lower than −0.50 eV. The steady hydrogen bonding networks between DMSO/$H_2O$ molecules and kaolinite layers in these cases are energetically more stable than the case with lower molar ratio of 0.25 (see Figure S2). As the molar ratio of hydrated DMSO continuously increases, the intercalation energy gradually becomes slightly lower. Moreover, the layer spacing of DMSO4/m$H_2O$/Kaol exceeds 1.15 nm, suggesting that stable kaolinite−DMSO intercalation complexes may not be formed. On the basis of the evaporation energy of $H_2O$ in each DMSO4/m$H_2O$/Kaol structure, some most stable structures are summarized in Table S4. These results strongly suggest that DMSO molecules can be stably intercalated in kaolinite when their loading amount is higher than 0.50, with or without water. And, the former case is energetically slightly more favorable. Furthermore, the partially replacement of DMSO by $H_2O$ is also thermodynamically favored for DMSO molar ratio between 0.50 and 1.00. On the basis of this set of computational results, we propose two mechanisms for DMSO intercalation in kaolinite. Specifically, one mechanism features direct intercalation of DMSO molecules at 1.00 mol/unit (Figure 3a); the other mechanism is intercalation of hydrated DMSO/$H_2O$ complex involving interlayer water molecules at 0.50 mol DMSO/unit (Figure 3a). It should be mentioned that, if we calculate the formation energy of DMSO and $H_2O$ in solvent case (eq S3), the intercalation energy of DMSO or $H_2O$ would be systematically increased by 0.58 or 0.68 eV, respectively, but the trends would remain the same.

Regardless the presence of water, interlayer confined DMSO interacts with kaolinite by binding at the Al−OH groups through hydrogen bonding. Such guest−host interactions effectively alter or rearrange the hydroxyl groups of kaolinite at its internal surface (inner−surface hydroxyls). The arrangement of inner−surface hydroxyl has been changed significantly due to the intercalation of DMSO (black circles) and the hydrogen bonding formation (Figures S1 and S2). The calculated hydrogen bonding specifics of DMSO1/Kaol are in good accordance with the data reported earlier listed in

**Table 1. Calculated Total Intercalation Energy (IE, in eV) and Intercalation Energy Per Molecule of DMSO/$H_2O$ (IE/Molecule) in DMSO and Water Intercalated Kaolinite[a]**

| intercalation | model | IE | IE/DMSO |
|---|---|---|---|
| Kaol + DMSO → kaolinite−DMSO | DMSO1/Kaol | 0.88 | 0.88 |
| | DMSO2/Kaol | −0.72 | −0.36 |
| | DMSO3/Kaol | −1.50 | −0.50 |
| | DMSO4/Kaol | −2.32 | −0.58 |
| | DMSO1/Kaol[b] | −0.14 | −0.14 |
| | DMSO2/Kaol[b] | −0.45 | −0.23 |
| | DMSO4/Kaol[b] | −0.96 | −0.24 |
| | DMSO/Kaol[c] | −0.42 (−1.29) | |
| Kaol + DMSO + water → kaolinite−DMSO−water | DMSO1/4$H_2O$/Kaol | −2.43 | −0.49 |
| | DMSO2/4$H_2O$/Kaol | −3.40 | −0.57 |
| | DMSO3/2$H_2O$/Kaol | −2.88 | −0.58 |
| | DMSO4/1$H_2O$/Kaol | −3.28 | −0.66 |
| Kaol + Me → kaolinite−Me | | −3.12[d] | |
| Kaol + Me + water → kaolinite−Me−water | | −4.38[d] | |
| Kaol + EG → kaolinite−EG | | −1.98[e] | |
| Kaol + EG + water → kaolinite−EG−water | | −3.01[e] | |

[a]Similar calculations for other intercalated molecules are also given. [b]DFT calculated results from ref 27. [c]B3LYP/3-21G (BSSE) results from ref 37. [d]Ref 22. [e]Ref 44. Me and EG are methanol and ethylene glycol, respectively.



https://doi.org/10.1021/acs.jpclett.1c02729
J. Phys. Chem. Lett. 2021, 12, 9973−9981

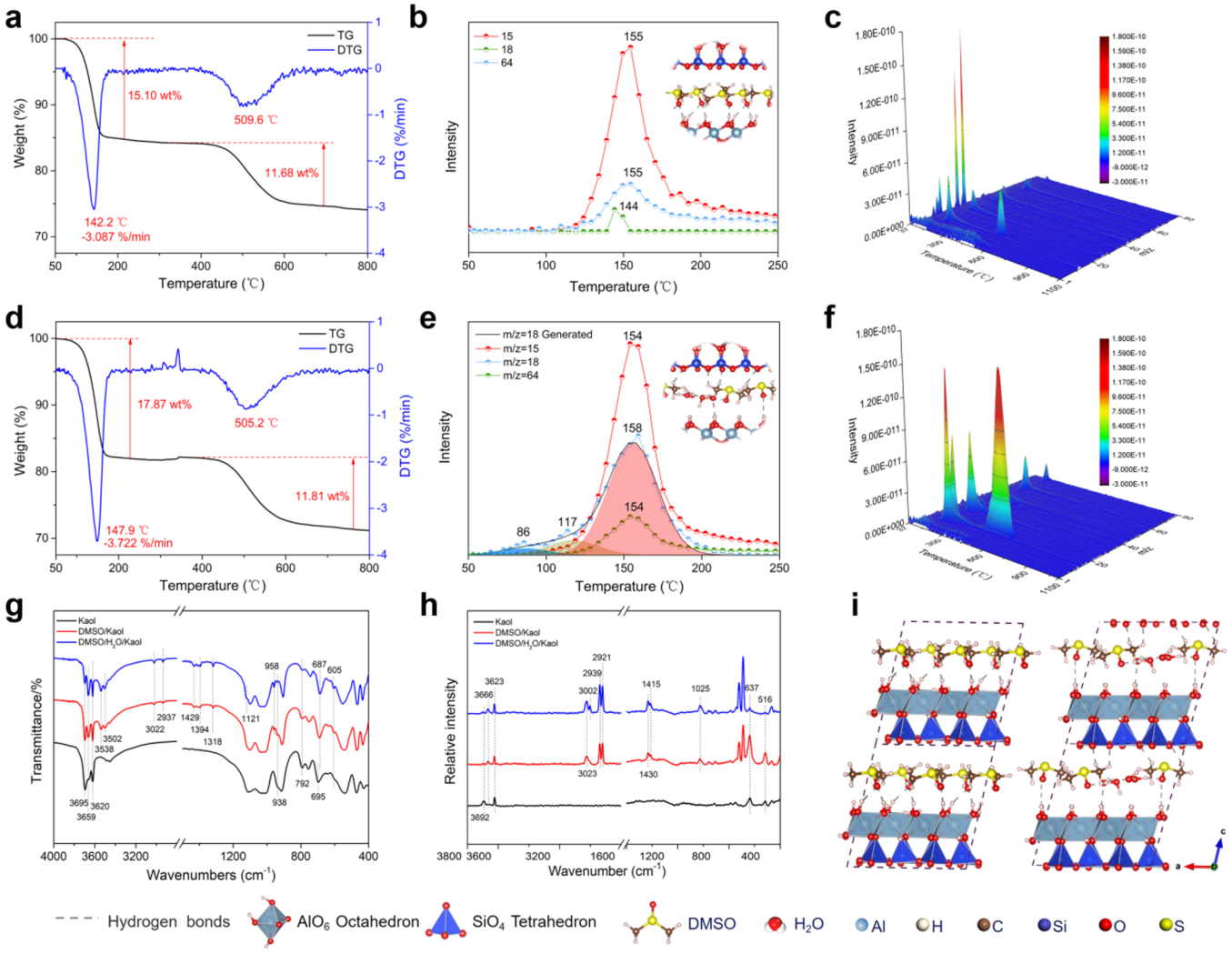


**Figure 4.** (a) TG and DTG curves, (b) $m/z$ = 15, 18, 64 MS curves, and (c) MS desorption yields of DMSO/Kaol. (d) TG and DTG, (e) $m/z$ = 15, 18, 64 MS curves, and (f) MS desorption yields of DMSO/$H_2O$/Kaol. Data were collected from 37 to 1100 °C at 10 °C/min under nitrogen flow. In panels c and f, highlighted atomic model of the interfacial structures are also presented. (g) FTIR and (h) Raman spectra of raw kaolinite and DMSO intercalated kaolinite. (i) Atomic models of DMSO/Kaol and DMSO/$H_2O$/Kaol.

Table S6. DFT-D accurately describes the bonding energetics of intercalation. Figure 3b–d present the details of hydrogen bonds for the kaolinite–DMSO intercalation complexes. The statistical summary of hydrogen bonds in Figure 3b suggests that, in general a shorter hydrogen bond length forms in DMSOn/$H_2O$/Kaol compared with its corresponding DMSOn/Kaol. Therefore, water promotes stronger DMSO intercalation in kaolinite. Moreover, the atom concentration profiles (see Figure 3c and d) suggest that the structure of DMSO/kaolinite complex is significantly unstable when water is present at a concentration of 1.00 mol DMSO per unit of kaolinite. This agrees well with our earlier observation that the *d*-spacing of DMSO4/$H_2O$/Kaol is greater than 1.12 nm. At the concentration range of 0.50–0.75 mol DMSO per unit of kaolinite, the concentrations of O atoms in water molecules and DMSO are approximately within the same range. This phenomenon highlights the cooperative effects of integrated DMSO and water complex in intercalation.

Thermal analysis using TG–MS provide both qualitative and quantitative information on thermal decomposition pathway and thermal stability of materials[43,45] In Figure S4, the total mass loss from raw kaolinite upon heating is 13.64 wt %, which is due to dehydration and dehydroxylation. The maximum mass loss is recorded at 519.2 °C. Figure 4a–c show the stepwise thermal decomposition pathway of DMSO/Kaol samples. For DMSO/Kaol, in step 1, the mass loss owing to DMSO removal (15.10 wt %) occurs at about 142.2 °C (see Figure 4a). The mass loss in step 2 (11.68 wt %), concluded at 509.8 °C, is due to dehydroxylation. For DMSO/$H_2O$/Kaol samples (see Figures 4d–f), the step 1 mass loss is because of simultaneous desorption of intercalated water and DMSO clusters at about 147.9 °C. In its step 2 weight loss at ~505.2 °C, the interplanar hydroxyl groups were detached (11.81 wt %). According to the TG data, the total amount of DMSO per unit structure of kaolinite of DMSO/Kaol and DMSO/$H_2O$/Kaol are 0.59 and 0.72, respectively. The decomposition temperature of sample with water intercalated, DMSO/$H_2O$/Kaol, appears to be slightly higher than that without water (DMSO/Kaol). The differences observed in thermal decomposition for DMSO/Kaol and DMSO/$H_2O$/Kaol, especially the significantly increased intercalation efficiency in the presence of water, agree well with the computational results, which highlight the critical role of water in promotion of DMSO intercalation.



https://doi.org/10.1021/acs.jpclett.1c02729
J. Phys. Chem. Lett. 2021, 12, 9973–9981

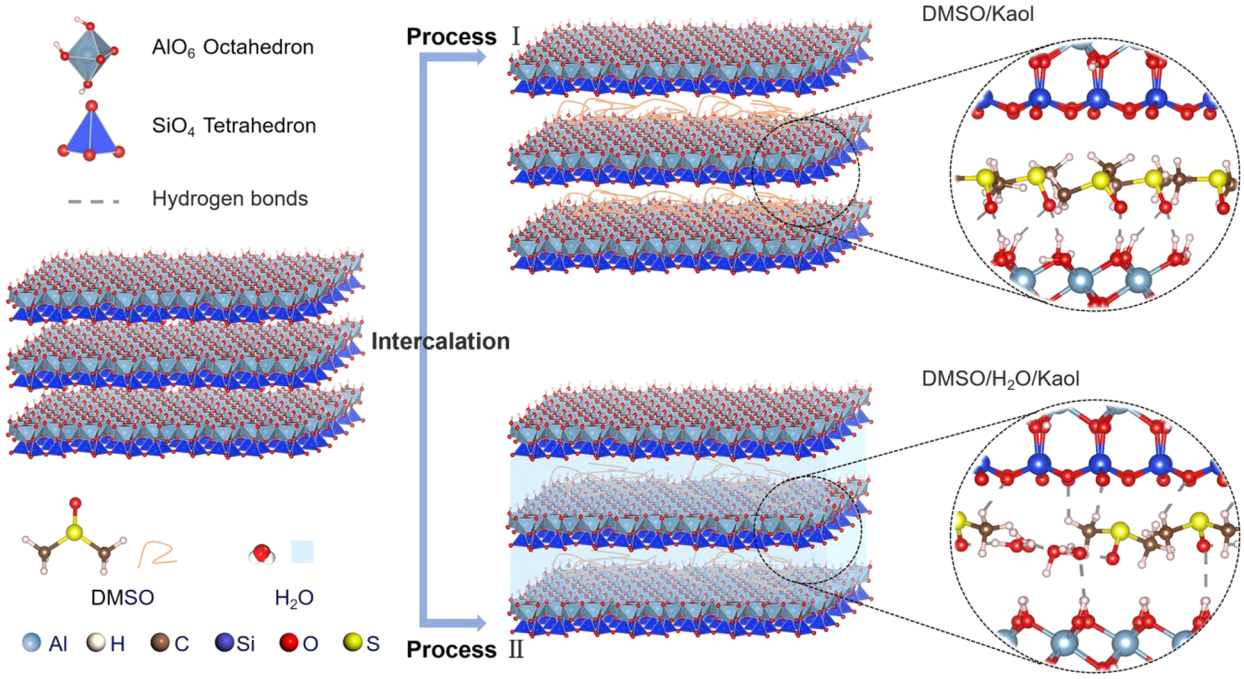


**Figure 5.** Illustration of DMSO intercalated kaolinite with and without the presence of water based on our computational and experimental results.

The evolved gas phase species in thermal decomposition of all samples were analyzed by TG−MS for $m/z$ ranging from 1 to 80 (see Figure 4c and f). Specifically, the major volatile products of thermal analysis were identified as $H_2O^+$ ($m/z$ = 18) from water, and $CH_3^+$ ($m/z$ = 15) and $SO_2^+$ ($m/z$ = 64) due to decomposition of DMSO. Table S8 lists the mass number ($m/z$), corresponding fragment, and the projected parent molecules. As shown in Figure 4b, complete decomposition of DMSO in DMSO/Kaol is achieved at 155 °C accompanied by slight dehydration at 144 °C, adsorbed moisture onto DMSO during the 8-day intercalation equilibrium under ambient condition. For DMSO/$H_2O$/Kaol (see the MS curve in Figure 4e), the maximum decomposition of DMSO is recorded at 154 °C. Meanwhile, water ($m/z$ = 18) is liberated at 86 and 117 °C (in cyan and violet, respectively), which is consistent with a previous report.[43] Notably, majority of water is desorbed and released simultaneously with DMSO at about 158 °C (in red), while the decomposition temperature of DMSO remains the same. Such phenomenon is strong evidence that the water molecules play a crucial role promoting effective intercalation of DMSO. This result could explain why DMSO−kaolinite complexes before 120 °C are different from those between 130 and 150 °C in Yariv's report.[35] Both theoretical and experimental results lead to the same conclusion: two distinctive mechanisms are needed for accurate description of DMSO intercalation in kaolinite considering the presence of water. Figure 4i presents a schematic illustration of the atomic models of DMSO/Kaol and DMSO/$H_2O$/Kaol.

FTIR spectra of DMSO/$H_2O$/Kaol, DMSO/Kaol, and raw kaolinite are plotted in Figure 4g, in which the interfacial bonding evolutions are characterized. The IR absorbance at 3695 and 3659 $cm^{-1}$ are attributed to vibrations of inner−surface hydroxyl groups of kaolinite.[46] Upon DMSO intercalation, the intensities of these two peaks are substantially edited due to the formation of hydrogen bonds with S═O groups of DMSO at the interplanar interfaces of kaolinite.[21,44] Additionally, two new peaks at 3538 and 3502 $cm^{-1}$ are observed in samples with intercalated DMSO molecules. Some earlier reports attributed these peaks to the stretching frequencies of inner−surface hydroxyls of kaolinite after hydrogen bond formation with S═O groups,[24,26] while others assigned them to hydroxyl stretching frequencies of water in the intercalation complexes. Water is considered to intercalated with DMSO in kaolinite either deliberately or adventitiously.[47,28] According to our theoretical calculations and TG-MS data, we agree with the studies concluding that H bonds at S═O residues. The IR absorption at 3620 $cm^{-1}$ from the inner hydroxyl groups[33] is not significantly perturbed. Instead, it presents slightly increased intensity accompanied by the guest species, DMSO, and water, in the interlayer space. The relative concentration of the inner hydroxyl groups nearly retains (see Figure 3c and d). The band at 1121 $cm^{-1}$ corresponds to blue-shift of the Si−O bond stretching vibrations that only observed for DMSO/$H_2O$/Kaol (see Figure 4g). This indicates that when water enhances the interactions between DMSO and the Si−O surface of kaolinite (see Figures 4e and i). Moreover, according to the study by Yariv and Lapides,[35] the perturbation band at 1121 $cm^{-1}$ is owing to H-bonds because of hydration. More specifically, it is very likely that water molecules fill the gap space linking the guest (DMSO) and the host (kaolinite) and enhancing the interactions between clay−O−plane and intercalated DMSO molecules.[35] After DMSO intercalation, the band at 938 $cm^{-1}$ assigned to Al−OH bending is blue-shifted to 958 $cm^{-1}$. Meanwhile, the signal at 792 $cm^{-1}$ attributed to out of phase stretching of Al−OH tends to be weaken, and the peak at 687 $cm^{-1}$ due to Al−OH symmetric vibration[34] is red-shifted to 695 $cm^{-1}$. These IR peaks detail the bonding evolutions of hydroxyl groups at the inner surface of kaolinite upon DMSO intercalation, which leads to strong hydrogen bonds formation between the guest, DMSO molecules, and Al−OH of kaolinite host with and without hydration. Moreover, the IR spectra suggest that the Si−O band of kaolinite is only significantly


https://doi.org/10.1021/acs.jpclett.1c02729
J. Phys. Chem. Lett. 2021, 12, 9973−9981

impacted for DMSO intercalation in the presence of water. Such phenomenon is consistent with our computational results. As demonstrated in Figure 4i, when both water and DMSO are intercalated, effective and strong hydrogen bonds formation is facilitated for the DMSO−water−kaolinite guest−host system, whose interaction energy is more exothermic than that of DMSO/Kaol.

Figure 4h shows the Raman spectra of DMSO intercalated kaolinite and untreated kaolinite. The band at 3623 $cm^{-1}$ is attributed to the inner hydroxyl stretching region;[48] the 3666 $cm^{-1}$ band is attributed to the inner surface hydroxyls; and the band at 3692 $cm^{-1}$ arises from the inner surface hydroxyls of kaolinite. The intensity variation of these bands arises from perturbations of these hydroxyls by formation of hydrogen bonds with DMSO. Raman bands at 2921, 2939, 3002, and 3023 $cm^{-1}$ are due to the splitting of the C−H symmetric and antisymmetric stretching vibrations of DMSO.[25] The in-plane methyl bending of DMSO lead to two Raman bands at 1415 and 1430 $cm^{-1}$. The peaks at 516 and 637 $cm^{-1}$ assigned to Al−OH of kaolinite are altered after intercalation of DMSO,[49] and the intensities of these peaks of DMSO/Kaol are much stronger than those of DMSO/$H_2O$/Kaol. Additionally, these bands were also reported to be edited under the presence of interlayer confined water for kaolinite.[50] The Raman spectra suggest that the water molecules are primarily adsorbed on the interplanar surfaces of kaolinite linking DMSO and the Al−OH groups of kaolinite. Figure 5 illustrates the details of bonding specifics and guest−host interactions for DMSO intercalated in kaolinite with and without hydration, which highlights the major outcome of our study−two intercalation mechanisms based on integrated DFT-D theoretic prediction and experimental validation.

Integrating theoretical and experimental studies, we reveal the critical role of water molecules in thermodynamically promoting efficient intercalation of DMSO in kaolinite. First, DFT-D calculations provide insight into the atomic scale structures and energetics of kaolinite−DMSO intercalation complexes. When the DMSO loading is 0.75−1.00 mol per unit kaolinite, the stable intercalation configurations are achieved owing to sufficient contribution from DMSO−kaolinite hydrogen bonds, which thermodynamically minimize the total energy of the system. In contrast, intercalated water molecules within the interplanar space of kaolinite result in synergistic effect between DMSO and kaolinite surface, which stabilize the DMSO−water−kaolinite guest−host system at a lower DMSO loading. In other words, hydration is energetically favorable, which promotes intercalation by formation of hydrogen bonded DMSO clusters that enables stronger guest−host interactions. Moreover, experimental methods, including FTIR, Raman, and TG-MS, were used to validate the proposed mechanisms, which confirmed the role of water molecules in aiding DMSO intercalation. In sum, our study elucidates the mechanisms of DMSO intercalation in kaolinite, in which the crucial role of interlayer hydration is highlighted. We expect that hydration engineering may be employed to fine-tune the intercalation and exfoliation of 2D materials for development of new energy storage materials, catalytic materials and nanohybrid materials.

## ■ ASSOCIATED CONTENT

### Supporting Information

Detailed description of the materials synthesis and calculation conditions. The Supporting Information is available free of charge at https://pubs.acs.org/doi/10.1021/acs.jpclett.1c02729.

Additional structural information and intercalation energy, surface area, XRD, SEM, and TG (PDF)

## ■ AUTHOR INFORMATION


### Corresponding Authors

**Liangjie Fu** − *Hunan Key Lab of Mineral Materials and Application, School of Minerals Processing and Bioengineering, Central South University, Changsha 410083, China; Engineering Research Center of Nano-Geomaterials of Ministry of Education, China University of Geosciences, Wuhan 430074, China; Faculty of Materials Science and Chemistry, China University of Geosciences, Wuhan 430074, China*; Phone: 86-731-88830549; Email: franch@csu.edu.cn; Fax: 86-731-88710804

**Huaming Yang** − *Hunan Key Lab of Mineral Materials and Application, School of Minerals Processing and Bioengineering, Central South University, Changsha 410083, China; Engineering Research Center of Nano-Geomaterials of Ministry of Education, China University of Geosciences, Wuhan 430074, China; Faculty of Materials Science and Chemistry, China University of Geosciences, Wuhan 430074, China*; orcid.org/0000-0002-3097-2850; Email: hmyang@csu.edu.cn, hm.yang@cug.edu.cn

### Authors

**Jie Wang** − *Hunan Key Lab of Mineral Materials and Application, School of Minerals Processing and Bioengineering, Central South University, Changsha 410083, China*

**Xiaochao Zuo** − *Engineering Research Center of Nano-Geomaterials of Ministry of Education, China University of Geosciences, Wuhan 430074, China; Faculty of Materials Science and Chemistry, China University of Geosciences, Wuhan 430074, China*

**Di Wu** − *Alexandra Navrotsky Institute for Experimental Thermodynamics, Washington State University, Pullman, Washington 99163, United States; The Gene and Linda Voiland School of Chemical Engineering and Bioengineering and Department of Chemistry, Washington State University, Pullman, Washington 99163, United States; Materials Science and Engineering, Washington State University, Pullman, Washington 99164, United States*; orcid.org/0000-0001-6879-321X

Complete contact information is available at: https://pubs.acs.org/10.1021/acs.jpclett.1c02729


### Notes

The authors declare no competing financial interest.

## ■ ACKNOWLEDGMENTS

This work was supported by the National Science Fund for Distinguished Young Scholars (51225403), the National Natural Science Foundation of China (52042403), the Strategic Priority Research Program of Central South University (ZLXD2017005), the Hunan Provincial Science and Technology Project (2018WK4023) and the Fundamental Research Funds for the Central Universities, China University of Geosciences (Wuhan). D.W. acknowledges the institutional funds from the Gene and Linda Voiland School of Chemical Engineering and Bioengineering and Alexandra Navrotsky

Institute for Experimental Thermodynamics at Washington State University.

## REFERENCES


(1) Nicolosi, V.; Chhowalla, M.; Kanatzidis, M. G.; Strano, M. S.; Coleman, J. N. Liquid Exfoliation of Layered Materials. *Science* **2013**, *340* (6139), 1226419.

(2) Coleman, J. N.; Lotya, M.; O'Neill, A.; Bergin, S. D.; King, P. J.; Khan, U.; Young, K.; Gaucher, A.; De, S.; Smith, R. J.; et al. Two-Dimensional Nanosheets Produced by Liquid Exfoliation of Layered Materials. *Science* **2011**, *331* (6017), 568−571.

(3) Ogawa, M.; Kuroda, K. Photofunctions of Intercalation Compounds. *Chem. Rev.* **1995**, *95* (2), 399−438.

(4) Toma, L. M.; Gengler, R. Y. N.; Cangussu, D.; Pardo, E.; Lloret, F.; Rudolf, P. New Magnetic Thin Film Hybrid Materials Built by the Incorporation of Octanickel(II)-Oxamato Clusters between Clay Mineral Platelets. *J. Phys. Chem. Lett.* **2011**, *2* (16), 2004−2008.

(5) Laipan, M.; Xiang, L.; Yu, J.; Martin, B. R.; Zhu, R.; Zhu, J.; He, H.; Clearfield, A.; Sun, L. Layered Intercalation Compounds: Mechanisms, New Methodologies, and Advanced Applications. *Prog. Mater. Sci.* **2020**, *109*, 100631.

(6) Dedzo, G. K.; Detellier, C. Clay Minerals-Ionic Liquids, Nanoarchitectures, and Applications. *Adv. Funct. Mater.* **2018**, *28* (27), 1703845.

(7) Chiu, C. W.; Lin, J. J. Self-Assembly Behavior of Polymer-Assisted Clays. *Prog. Polym. Sci.* **2012**, *37* (3), 406−444.

(8) Gardolinski, J. E.; Carrera, L. C. M.; Cantão, M. P.; Wypych, F. Layered Polymer-Kaolinite Nanocomposites. *J. Mater. Sci.* **2000**, *35* (12), 3113−3119.

(9) Sun, L.; O'Reilly, J. Y.; Kong, D.; Su, J. Y.; Boo, W. J.; Sue, H. J.; Clearfield, A. The Effect of Guest Molecular Architecture and Host Crystallinity upon the Mechanism of the Intercalation Reaction. *J. Colloid Interface Sci.* **2009**, *333* (2), 503−509.

(10) Hu, H.; Martin, J. C.; Xiao, M.; Southworth, C. S.; Meng, Y.; Sun, L. Immobilization of Ionic Liquids in Layered Compounds via Mechanochemical Intercalation. *J. Phys. Chem. C* **2011**, *115* (13), 5509−5514.

(11) Boo, W. J.; Sun, L.; Liu, J.; Clearfield, A.; Sue, H. J. Effective Intercalation and Exfoliation of Nanoplatelets in Epoxy via Creation of Porous Pathways. *J. Phys. Chem. C* **2007**, *111* (28), 10377−10381.

(12) Tunney, J. J.; Detellier, C. Aluminosilicate Nanocomposite Materials. Poly(Ethylene Glycol)-Kaolinite Intercalates. *Chem. Mater.* **1996**, *8* (4), 927−935.

(13) Li, C.; Huang, Y.; Dong, X.; Sun, Z.; Duan, X.; Ren, B.; Zheng, S.; Dionysiou, D. D. Highly Efficient Activation of Peroxymonosulfate by Natural Negatively-Charged Kaolinite with Abundant Hydroxyl Groups for the Degradation of Atrazine. *Appl. Catal., B* **2019**, *247*, 10−23.

(14) Zhao, Q.; Fu, L.; Jiang, D.; Ouyang, J.; Hu, Y.; Yang, H.; Xi, Y. Nanoclay-Modulated Oxygen Vacancies of Metal Oxide. *Commun. Chem.* **2019**, *2* (1), 11.

(15) Liu, S.; Yan, Z.; Fu, L.; Yang, H. Hierarchical Nano-Activated Silica Nanosheets for Thermal Energy Storage. *Sol. Energy Mater. Sol. Cells* **2017**, *167*, 140−149.

(16) Peng, K.; Fu, L.; Li, X.; Ouyang, J.; Yang, H. Applied Clay Science Stearic Acid Modified Montmorillonite as Emerging Micro-capsules for Thermal Energy Storage. *Appl. Clay Sci.* **2017**, *138*, 100−106.

(17) Ofili, N. E. R.; Thetford, A.; Kaltsoyannis, N. Adsorption of U(VI) on Stoichiometric and Oxidised Mackinawite: A DFT Study. *Environ. Sci. Technol.* **2020**, *54* (11), 6792−6799.

(18) Murugesan, S.; Scheibel, T. Copolymer/Clay Nanocomposites for Biomedical Applications. *Adv. Funct. Mater.* **2020**, *30* (17), 1908101.

(19) Long, M.; Zhang, Y.; Huang, P.; Chang, S.; Hu, Y.; Yang, Q.; Mao, L.; Yang, H. Emerging Nanoclay Composite for Effective Hemostasis. *Adv. Funct. Mater.* **2018**, *28* (10), 1704452.

(20) Bergaya, F.; Lagaly, G. *Handbook of Clay Science*; Elsevier: Amsterdam, 2013.

(21) Zhang, S.; Liu, Q.; Cheng, H.; Gao, F.; Liu, C.; Teppen, B. J. Mechanism Responsible for Intercalation of Dimethyl Sulfoxide in Kaolinite: Molecular Dynamics Simulations. *Appl. Clay Sci.* **2018**, *151*, 46−53.

(22) Cheng, H.; Hou, X.; Liu, Q.; Li, X.; Frost, R. L. New Insights into the Molecular Structure of Kaolinite-Methanol Intercalation Complexes. *Appl. Clay Sci.* **2015**, *109*, 55−63.

(23) Olejnik, S.; Aylmore, L. A. G.; Posner, A. M.; Quirk, J. P. Infrared Spectra of Kaolin Mineral-Dimethyl Sulfoxide Complexes. *J. Phys. Chem.* **1968**, *72* (1), 241−249.

(24) Makó, É.; Kovács, A.; Kristóf, T. Influencing Parameters of Direct Homogenization Intercalation of Kaolinite with Urea, Dimethyl Sulfoxide, Formamide, and N-Methylformamide. *Appl. Clay Sci.* **2019**, *182*, 105287.

(25) Frost, R. L.; Kristof, J.; Paroz, G. N.; Tran, T. H.; Kloprogge, J. T. The Role of Water in the Intercalation of Kaolinite with Potassium Acetate. *J. Colloid Interface Sci.* **1998**, *204* (2), 227−236.

(26) Li, X.; Cui, X.; Wang, S.; Wang, D.; Li, K.; Liu, Q.; Komarneni, S. Methoxy-Grafted Kaolinite Preparation by Intercalation of Methanol: Mechanism of Its Structural Variability. *Appl. Clay Sci.* **2017**, *137*, 241−248.

(27) Frost, R. L.; Kristof, J.; Horvath, E.; Kloprogge, J. T. Deintercalation of Dimethylsulfoxide Intercalated Kaolinites - a DTA/TGA and Raman Spectroscopic Study. *Thermochim. Acta* **1999**, *327* (1−2), 155−166.

(28) Frost, R. L.; Kristof, J.; Horvath, E.; Kloprogge, J. T. Effect of Water on the Formamide-Intercalation of Kaolinite. *Spectrochim. Acta, Part A* **2000**, *56* (9), 1711−1729.

(29) Cheng, Z. L.; Cao, B. C.; Liu, Z. Study on Intercalation in Layered Structure of Halloysite Nanotubes (HNTs). *Micro Nano Lett.* **2019**, *14* (5), 585−589.

(30) Olejnik, S.; Posner, A. M.; Quirk, J. P. The Intercalation of Polar Organic Compounds into Kaolinite. *Clay Miner.* **1970**, *8* (4), 421−434.

(31) Ho, T. A.; Criscenti, L. J.; Greathouse, J. A. Revealing Transition States during the Hydration of Clay Minerals. *J. Phys. Chem. Lett.* **2019**, *10* (13), 3704−3709.

(32) Takenawa, R.; Komori, Y.; Hayashi, S.; Kawamata, J.; Kuroda, K. Intercalation of Nitroanilines into Kaolinite and Second Harmonic Generation. *Chem. Mater.* **2001**, *13* (10), 3741−3746.

(33) Frost, R. L.; Kristof, J.; Paroz, G. N.; Kloprogge, J. T. Molecular Structure of Dimethyl Sulfoxide Intercalated Kaolinites. *J. Phys. Chem. B* **1998**, *102* (43), 8519−8532.

(34) Abou-El-Sherbini, K. S.; Elzahany, E. A. M.; Wahba, M. A.; Drweesh, S. A.; Youssef, N. S. Evaluation of Some Intercalation Methods of Dimethylsulfoxide onto HCl-Treated and Untreated Egyptian Kaolinite. *Appl. Clay Sci.* **2017**, *137*, 33−42.

(35) Yariv, S.; Lapides, I. Thermo-Infrared-Spectroscopy Analysis of Dimethylsulfoxide-Kaolinite Intercalation Complexes. *J. Therm. Anal. Calorim.* **2008**, *94* (2), 433−440.

(36) Zhang, S.; Liu, Q.; Cheng, H.; Zeng, F. Combined Experimental and Theoretical Investigation of Interactions between Kaolinite Inner Surface and Intercalated Dimethyl Sulfoxide. *Appl. Surf. Sci.* **2015**, *331*, 234−240.

(37) Michalková, A.; Tunega, D.; Nagy, L. T. Theoretical Study of Interactions of Dickite and Kaolinite with Small Organic Molecules. *J. Mol. Struct.: THEOCHEM* **2002**, *581* (1−3), 37−49.

(38) Michalková, A.; Tunega, D. Kaolinite: Dimethylsulfoxide Intercalate - A Theoretical Study. *J. Phys. Chem. C* **2007**, *111* (30), 11259−11266.

(39) Korsun, O. M.; Kalugin, O. N.; Prezhdo, O. V. Control of Carbon Nanotube Electronic Properties by Lithium Cation Intercalation. *J. Phys. Chem. Lett.* **2014**, *5* (23), 4129−4133.

(40) Mbey, J.A.; Thomas, F.; Ngally Sabouang, C.J.; Liboum; Njopwouo, D. An Insight on the Weakening of the Interlayer Bonds in a Cameroonian Kaolinite through DMSO Intercalation. *Appl. Clay Sci.* **2013**, *83-84*, 327−335.




https://doi.org/10.1021/acs.jpclett.1c02729
J. Phys. Chem. Lett. 2021, 12, 9973−9981

(41) Tunega, D.; Bučko, T.; Zaoui, A. Assessment of Ten DFT Methods in Predicting Structures of Sheet Silicates: Importance of Dispersion Corrections. *J. Chem. Phys.* **2012**, *137* (11), 114105.
(42) Fu, L.; Yang, H.; Tang, A.; Hu, Y. Engineering a Tubular Mesoporous Silica Nanocontainer with Well-Preserved Clay Shell from Natural Halloysite. *Nano Res.* **2017**, *10* (8), 2782−2799.
(43) Zhang, S.; Liu, Q.; Gao, F.; Ma, R.; Wu, Z.; Teppen, B. J. Interfacial Structure and Interaction of Kaolinite Intercalated with N-Methylformamide Insight from Molecular Dynamics Modeling. *Appl. Clay Sci.* **2018**, *158*, 204−210.
(44) Hou, X. J.; Li, H.; Li, S.; He, P. Theoretical Study of the Intercalation Behavior of Ethylene Glycol on Kaolinite. *J. Phys. Chem. C* **2014**, *118* (45), 26017−26026.
(45) Hu, H.; Martin, J. C.; Zhang, M.; Southworth, C. S.; Xiao, M.; Meng, Y.; Sun, L. Immobilization of Ionic Liquids in -Zirconium Phosphate for Catalyzing the Coupling of $CO_2$ and Epoxides. *RSC Adv.* **2012**, *2* (9), 3810−3815.
(46) Frost, R. L.; Locos, O. B.; Kristof, J.; Kloprogge, J. T. Infrared Spectroscopic Study of Potassium and Cesium Acetate-Intercalated Kaolinites. *Vib. Spectrosc.* **2001**, *26* (1), 33−42.
(47) Elbokl, T. A.; Detellier, C. Intercalation of Cyclic Imides in Kaolinite. *J. Colloid Interface Sci.* **2008**, *323* (2), 338−348.
(48) Pajcini, V.; Dhamelincourt, P. Raman Study of OH-Stretching Vibrations in Kaolinite at Low Temperature. *Appl. Spectrosc.* **1994**, *48* (5), 638−641.
(49) Smrčok, L.; Tunega, D.; Ramirez-Cuesta, A. J.; Scholtzová, E. The Combined Inelastic Neutron Scattering and Solid State DFT Study of Hydrogen Atoms Dynamics in a Highly Ordered Kaolinite. *Phys. Chem. Miner.* **2010**, *37* (8), 571−579.
(50) Johnston, C. T.; Sposito, G.; Bocian, D. F.; Birge, R. R. Vibrational Spectroscopic Study of the Interlamellar Kaolinite-Dimethyl Sulfoxide Complex. *J. Phys. Chem.* **1984**, *88* (24), 5959−5964.


https://doi.org/10.1021/acs.jpclett.1c02729
*J. Phys. Chem. Lett.* 2021, 12, 9973−9981